

Pairing Mechanism in Hund's Metal Superconductors and the Universality of the Superconducting Gap to Critical Temperature Ratio

Tsung-Han Lee,¹ Andrey Chubukov,² Hu Miao,³ and Gabriel Kotliar^{4,3}

¹*Physics and Astronomy Department, Rutgers University, Piscataway, New Jersey 08854, USA*

²*School of Physics and Astronomy, University of Minnesota, Minneapolis, Minnesota 55455, USA*

³*Brookhaven National Laboratory, Upton, New York 11973, USA*

⁴*Physics and Astronomy Department, Rutgers University, Piscataway, NJ 08854, USA*

(Dated: November 8, 2021)

We analyze a simple model containing the physical ingredients of a Hund's metal, the local spin fluctuations with power-law correlators, $(\Omega_0/|\Omega|)^\gamma$, with γ greater than one, interacting with electronic quasiparticles. While the critical temperature and the gap change significantly with varying parameters, the $2\Delta_{\max}/k_B T_c$ remains close to twice the BCS value in agreement with experimental observations in the iron-based superconductors (FeSC).

Introduction The discovery of superconductivity in iron-based materials¹ opened a new area of research in the field of superconducting materials. There are by now many families of materials which are based on tetrahedrally coordinated irons to pnictides and chalcogenides, with different separating layers in between. For a review, see Refs. 2 and 3. Photoemission studies have shown that some of these compounds have bands which are well described by the standard density functional theory with small renormalizations, while in others, the mass renormalizations are larger than ten. Hence, it is agreed upon that in this class of compounds the strength of the correlation varies substantially. On the other hand, there is no agreement on the type of correlation, which is attributed to Mott⁴ or Hund's physics^{5–7}.

Thinking of the iron pnictides as Hund's metals presents a scenario, in which the physics governing the behavior of different materials is the same, but the correlations are sensitive to the filling of the shell and the height of the pnictogen or chalcogen ligand⁸. A deeper understanding of Hund's metal physics shows that the normal state above the superconducting transition has a broad intermediate region of temperatures characterized by orbital spin separation, whereby the spin excitations are quasi-atomic-like, while the orbital excitations are fully itinerant^{9–11}. Thus, the Hund's metal behavior exists in a temperature range below the Kondo scale of the orbital degrees of freedom T_K^{orb} and above the Kondo scale of the spin degrees of freedom T_K^{sp} , below which the Fermi liquid holds¹¹.

Whether a Hund's metal becomes a superconductor at high temperatures is expected to depend on many microscopic details such as the shape of the Fermi surfaces of the electrons, the dispersion of the spin excitations, and how they are coupled to electrons^{12,13}. Hence the superconducting critical temperature is not a universal quantity, much like a coherence-incoherence crossover where a Fermi liquid emerges from a Hund's metal state.

In this Letter, we point out a universal aspect of superconductivity, which emerges from a Hund's metal state at higher temperatures – we argue that while T_c and the maximum value of the superconducting gap at $T = 0$, Δ_{\max} , are material-dependent, their ratio $2\Delta_{\max}/T_c$ is

material-independent universal number. We show that this is the case if the pairing in a Hund's metal is mediated by quasilocal spin excitations. As the normal state of a Hund's metal, involves incomplete screening, it is characterized by a power-law behavior of all the physical quantities^{5,9–11}. In particular, the susceptibility of local spin fluctuations has a power law dependence above a characteristic Kondo scale. While an analytic theory of such power-law behavior is not yet available, the numerical studies and physical considerations clearly indicate that the spin susceptibility follows $\chi(\Omega) \propto 1/|\Omega|^\gamma$ with $\gamma > 1$ ¹¹. Here we show that, when such $\chi(\Omega)$ mediates superconductivity emerging from the Hund's metal state, the ratio $2\Delta_{\max}/k_B T_c$ is a universal, γ -dependent number, which for $\gamma > 1$ is substantially larger than the BCS value. Universality here means that this number does not depend on the strength of the coupling to magnetic fluctuations, while T_c and Δ_{\max} vary strongly with the strength of fermion-boson coupling.

These results are in agreement with the conclusions of recent experiments on FeSC which addressed this question from an experimental perspective. By measuring the gap and the critical temperature in LiFeAs and FeTe_{0.55}Se_{0.45}, Miao *et al.* established¹⁴ that in both systems $2\Delta_{\max}/k_B T_c \sim 7.2$, despite the fact that the electronic structures are different. The previous study on the spin resonance also found a universal ratio, $\Omega_{\text{res}}/k_B T_c$ ¹⁵. This last observation is consistent with the universality of $2\Delta_{\max}/k_B T_c$ if Ω_{res} scales with Δ_{\max} as numerous studies of spin resonance suggested¹⁶.

Hund's metals are not confined to the iron-based superconductors and are in fact very common. Sr₂RuO₄ is a prime example of Hund's metal^{17–21}. However, for Sr₂RuO₄, its T_K^{sp} is much higher than its superconducting temperature¹⁸. Consequently, the normal state above the superconducting transition is already a Fermi liquid instead of a Hund's metal as in FeSCs. Therefore, our theory does not apply there.

Model To describe superconductivity in Hund's metals we use the γ -model, which was introduced in the context of superconductivity near a quantum critical point^{22–31}. Namely, we assume that interaction between fermions is

mediated by a local spin susceptibility $\chi(\Omega) \propto 1/|\Omega|^\gamma$ ³². This interaction simultaneously gives rise to pairing and frequency-dependent fermionic self-energy $\Sigma(\omega)$. The γ -model ignores many of the complications of a realistic description of the iron pnictide superconductors: a) its multiband and multiorbital nature, b) multiple Fermi surfaces, c) orbital-induced gap variation along the Fermi surfaces and the variation of the phase and magnitude of a superconducting order parameter between different Fermi surfaces, d) fine features in the dynamical structure factor of spin fluctuations (see Refs. 7, 33–37 for recent reviews). It retains, however, two essential features, the superlinear divergence of the local spin susceptibility at intermediate frequencies, and the coupling of quasilocalized spins to fermionic quasiparticles. We argue that this is the essential ingredient to understand the results of Ref. [14] that a) the ratio of $2\Delta_{\max}/k_B T_c$ is much larger than in BCS theory and b) it does not vary between different materials, as opposed to T_c and Δ_{\max} , both of which are material dependent.

The expressions for T_c and Δ_{\max} in the γ -model are obtained by solving the set of Eliashberg equations^{24,26,27,31,32,38} for the pairing vertex $\Phi(\omega_n)$ and fermionic self-energy $\Sigma(\omega_n)$ with a power-law form of the interaction:

$$\Sigma(\omega_n) = \pi T \sum_{\omega_m} \lambda(\omega_m - \omega_n) \frac{\omega_m + \Sigma(\omega_m)}{\sqrt{[\omega_m + \Sigma(\omega_m)]^2 + \Phi^2(\omega_m)}}, \quad (1)$$

$$\Phi(\omega_n) = \pi T \sum_{\omega_m} \lambda(\omega_m - \omega_n) \frac{\Phi(\omega_m)}{\sqrt{[\omega_m + \Sigma(\omega_m)]^2 + \Phi^2(\omega_m)}}, \quad (2)$$

where

$$\lambda(\Omega) = \left(\frac{\Omega_0}{|\Omega|} \right)^\gamma, \quad (3)$$

and Ω_0 determines the strength of fermion-boson coupling. The two Eliashberg equations can be partly factorized by introducing the pairing gap $\Delta(\omega_n) = \Phi(\omega_n)\omega_n/[\omega_n + \Sigma(\omega_n)]$ instead of $\Phi(\omega)$. With this substitution, the self-energy $\Sigma(\omega_n)$ drops from the equation for $\Delta(\omega)$. We have

$$\Delta(\omega_n) = \pi T \sum_{\omega_m} \frac{\lambda(\omega_m - \omega_n)}{\sqrt{\omega_m^2 + \Delta^2(\omega_m)}} (\Delta(\omega_m) - \Delta(\omega_n) \frac{\omega_m}{\omega_n}). \quad (4)$$

The $\lambda(\Omega)$ diverges at $\Omega = 0$, when $\omega_n = \omega_m$. However, the term in the bracket in the rhs of Eq. 4 becomes zero at $\omega_n = \omega_m$, which cancels out the divergence. Hence, Eq. 4 is free from singularities at any finite T . The equation on $\Sigma(\omega)$ does depend on $\Delta(\Omega_n)$:

$$\Sigma(\omega_n) = \pi T \sum_{\omega_m} \lambda(\omega_m - \omega_n) \frac{\omega_m}{\sqrt{\omega_m^2 + \Delta^2(\omega_m)}}. \quad (5)$$

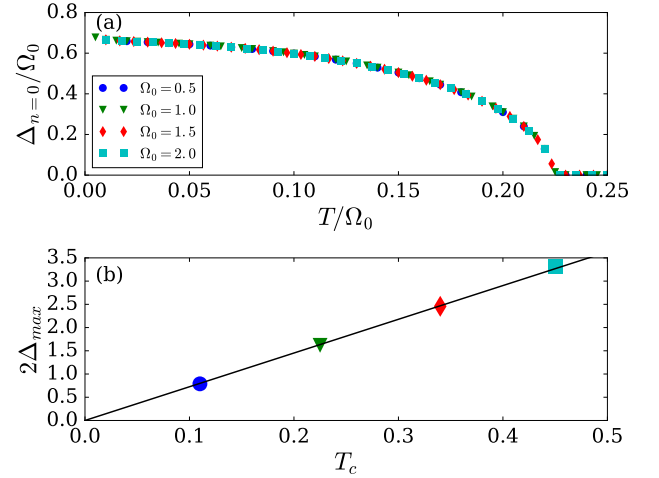


FIG. 1. (Color online) (a) The pairing gap at the first Matsubara frequency $\Delta_{n=0}$ as a function of temperature T for different pairing amplitudes Ω_0 at $\gamma = 1.2$. (b) The maximum gap Δ_{\max} and critical temperature T_c for various pairing amplitudes Ω_0 at $\gamma = 1.2$. The black solid line is the linear fit to the slope, $2\Delta_{\max}/T_c = 7.2$, corresponding to the experimental value observed in FeSC.

Because of semifactorization, one has to solve first Eq. 4 for $\Delta(\omega_n)$, substitute the result into Eq. 5 and obtain $\Sigma(\omega_n)$.

In quantum-critical theories, $\gamma = 2$ corresponds to the strong coupling limit of electron-phonon interaction³⁹, $\gamma = 1/2$ describes pairing by antiferromagnetic spin fluctuations in 2D^{22,24,25}, $\gamma = 1/3$ describes pairing by a gauge field and ferromagnetic spin fluctuations in 2D^{30,40–44}, and $\gamma = 0+$ describes color superconductivity and pairing in 3D^{45,46}. The models with varying $\gamma < 1$ have also been analyzed^{26,27,29,31}. Here we use the fact that in a wide range of frequencies a Hund's metal is also characterized by a local susceptibility, $\chi(\Omega) \propto 1/|\Omega|^\gamma$, with γ greater than one³², and explore the consequences of such a model on the $2\Delta_{\max}/T_c$ ratio by numerically and analytically solving Eq. 3 and Eq. 4. We obtain $\Delta(\omega_m)$ on the Matsubara axis and convert it onto real axis by analytical continuation. We define Δ_{\max} at $T = 0.005\Omega_0$ as the frequency at which the density of states $N(\omega) \propto \text{Im}[\omega/(\Delta^2(\omega) - \omega^2)]$ jumps to a finite value, i.e., set $\Delta_{\max} = \Delta(\omega = \Delta_{\max})$.

The results Figure 1(a) shows our results of the pairing gap at the first Matsubara frequency, $\Delta_{n=0}$, as a function of temperature T for a given $\gamma = 1.2$. We see that $\Delta_{n=0}$, measured in units of the interaction strength Ω_0 , is a universal function of T/Ω_0 (i.e., the functional form does not depend on Ω_0). This can be seen directly from Eq. 4 by simultaneously rescaling $\Delta(\omega_n)$ and Matsubara frequencies $\omega_{n,m}$ by Ω_0 . For this particular γ we obtained $\Delta_{\max} = 0.69\Omega_0 \approx \Delta(\pm\pi T)$ and $T_c = 0.19\Omega_0$. The ratio $2\Delta_{\max}/T_c = 7.2$ is the universal number, independent of Ω_0 , as we explicitly show in Fig. 1(b). This universality is indeed the consequence of the fact that Ω_0 is the only energy scale in the problem. For a generic γ , we expect

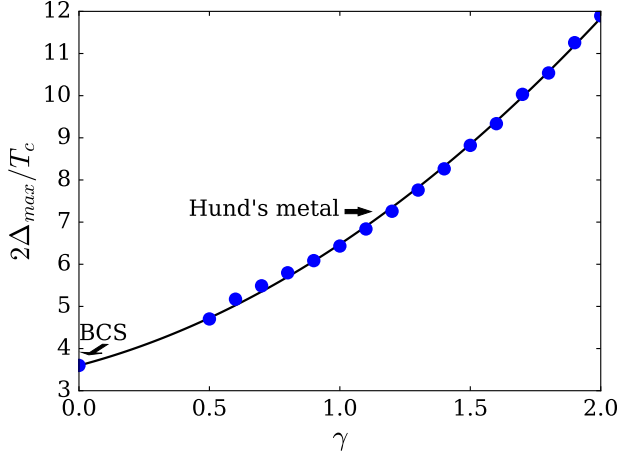


FIG. 2. (Color online) The ratio $2\Delta_{\max}/T_c$ as a function of γ . The arrows indicate the ratio $2\Delta_{\max}/T_c = 7.2$ ($\gamma \sim 1.2$) and 3.6 ($\gamma = 0$) corresponding to the ratio for FeSC and BCS. The black solid line is the fit to a parabola with $2\Delta_{\max}/T_c = 3.6 + 1.63\gamma + 1.24\gamma^2$.

$$T_c = A(\gamma)\Omega_0 \text{ and } \Delta_{\max} = B(\gamma)\Omega_0, \text{ i.e., } 2\Delta_{\max}/T_c = 2B(\gamma)/A(\gamma).$$

It is instructive to study how the ratio $2\Delta_{\max}/T_c$ varies with the exponent γ because different γ describe different pairing mechanisms. We show our numerical results for $2\Delta_{\max}/T_c$ for various γ in Fig. 2. The ratio, $2\Delta_{\max}/T_c$, increases with increasing γ in a parabolic fashion which can be extrapolated to the BCS ratio, $2\Delta_{\max}/T_c = 3.6$, at $\gamma \geq 0$. We found that the experimental $2\Delta_{\max}/T_c \sim 7.2$, reported by Miao *et al.*, is reproduced for $\gamma \sim 1.2$. Remarkably, this value of γ coincides with the exponent of the local spin susceptibility, obtained from the extensive numerical analysis of Hund's metal state in the three-band Hubbard model^{9,11}. This agreement is the strong argument that incoherent spin fluctuations, specific to a Hund's metal state, may indeed mediate superconductivity in FeSCs.

To get further insight into this issue, we now discuss how Δ_{\max} , T_c , and also fermionic $\Sigma(\omega_m)$ individually vary with γ . To get $T_c(\gamma)$ and self-energy near T_c , we follow^{26,27} and (a) solve for T at which the linearized gap equation (the one with infinitesimally small $\Delta(\omega_m)$) has the solution, and (b) solve Eq. 5 at $\Delta_n = 0$.

We show the result of numerical calculation of $\Sigma(\omega_n)$ in Fig. 3(a). Analytical reasoning shows²⁶ that, at large ω_n , $\Sigma(\omega_m)$ scales as $\omega_n^{1-\gamma}$ for $0 < \gamma < 1$ and saturates to $\Sigma(\omega_m) = [\Omega_0^\gamma/(2\pi T)^{\gamma-1}]\zeta(\gamma)$ for $\gamma > 1$, where $\zeta(\gamma)$ is the Riemann zeta function. Our numerical results fully reproduce this asymptotic behavior. In Fig. 3(b) we show the numerical result for the prefactor $A(\gamma)$ in the critical temperature, $T_c = A(\gamma)\Omega_0$. The analytical expression for $A(\gamma)$ has been obtained in Ref. 27 within large N approximation. An extension of that result to the physical case $N = 1$ yields $A(\gamma) = \frac{1}{2\pi}(1 + \frac{\delta_\gamma}{\gamma})$, where δ_γ is a number in the order of one ($\delta_{\gamma \gg 1} \approx 1/2$). Our

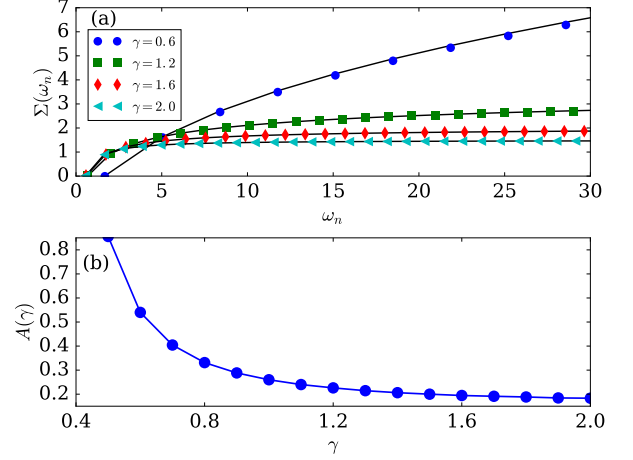


FIG. 3. (Color online) (a) The Matsubara self-energy $\Sigma(\omega_n)$ for different power γ , with $\Omega_0 = 1$ near critical temperature T_c . The black solid line is the analytic solution, from Moon and Chubukov²⁶. (b) The coefficient $A(\gamma)$ corresponding to the critical temperature $T_c = A(\gamma)\Omega_0$ as a function of power γ .

numerical result is consistent with this formula, particularly the increase of $A(\gamma)$ at smaller γ and the saturation of $A(\gamma)$ at $1/2\pi$ at larger γ (for $\gamma = 2$ we found $A(2) = 0.18$, in good agreement with Ref. 27).

At low temperatures, the pairing gap $\Delta(\omega_n)$, is no longer a small quantity. The linearization trick is no longer applicable, and we have to solve the full nonlinear gap equation for $\Delta(\omega_n)$ and convert the result to the real frequency axis. In Fig. 4 we show the results for the self-energy $\Sigma(\omega_n)$ and the prefactor $B(\gamma)$ in $\Delta_{\max} = B(\gamma)\Omega_0$, obtained from Eq. 5 using the solution of $\Delta(\omega_n)$, for $T = 0.005\Omega_0$. The self-energy $\Sigma(\omega)$ (Fig. 4(a)) scales linearly with ω_n at small frequencies, as expected in a Fermi liquid. The restoration of Fermi-liquid behavior is the known feedback effect from superconductivity, which, e.g., accounts for peak-dip-hump behavior in cuprate superconductors below T_c (see, e.g., Ref. [47]). In physical terms, this happens because a finite gap reduces quasiparticle scattering at low frequencies and makes low-energy states longer-lived. The slope of $\Sigma(\omega_n)$ at low frequency increases with increasing γ , indicating that correlations get stronger.

The behavior of $B(\gamma)$ is shown in Fig. 4(b). At small γ , $B(\gamma)$ decreases rather abruptly with increasing γ . At larger γ , $B(\gamma)$ passes through a minimum at $\gamma \sim 1.2$ and slowly increases for $\gamma > 1.2$. The ratio $2\Delta_{\max}/T_c$ (Fig. 2) is determined by the ratio between $B(\gamma)$ (Fig. 4(b)) and $A(\gamma)$ (Fig. 3(b)). At small γ , both $A(\gamma)$ and $B(\gamma)$ strongly evolve with γ , but the decrease of $B(\gamma)$ with increasing γ roughly follows the trend of $A(\gamma)$. As a result, the ratio $2B(\gamma)/A(\gamma)$ increases with increasing γ but varies not as strongly as $A(\gamma)$ and $B(\gamma)$. For larger $\gamma > 1.2$, $A(\gamma)$ saturates and the enhancement of $2\Delta_{\max}/T_c$ is due to the increase of $B(\gamma)$.

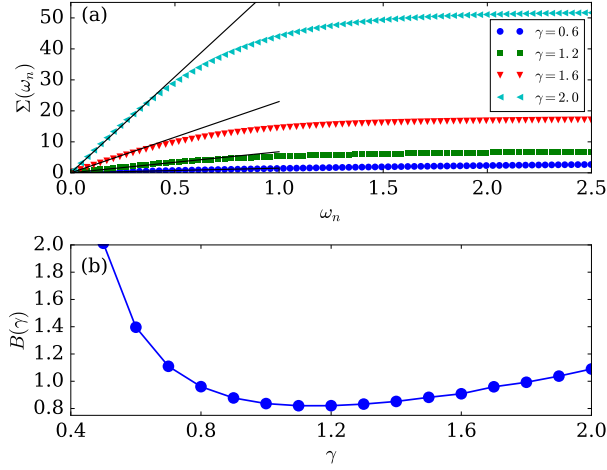


FIG. 4. (Color online) (a) The Matsubara self-energy $\Sigma(\omega_n)$ for different power γ at $\Omega_0 = 1$ and $T = 0.005\Omega_0$. The solid black lines indicate the low-frequency linear behavior. (b) The coefficient, $B(\gamma)$, corresponding to the maximum of the pairing gap $\Delta_{\max} = B(\gamma)\Omega_0$, as a function of the exponent γ .

Discussion Motivated by the theoretical understanding we reexamined $2\Delta_{\max}/T_c$ in other Fe-based superconductors. The data are summarized in Fig. 5. We see that they fall onto a single curve with the same slope $2\Delta_{\max}/T_c = 7.2 \pm 1$ as in LiFeAs and FeTe_{0.55}Se_{0.45}. This universality is the strong argument in favor of Hund's metal description with electronic (spin fluctuation) pairing mechanism. Remarkably, the data for FeSe monolayers fall on a different curve with a smaller $2\Delta_{\max}/T_c = 4 \pm 0.5$. This is consistent with the idea that in these systems the pairing may be mediated by electron-phonon interaction^{48–51}.

FeSCs are members of a broad class of unconventional superconductors, which also include copper oxides, heavy fermion metals, and the organic charge-transfer salts. The normal state of all these superconductors satisfies the criterion of bad metals, superconductivity appears near an antiferromagnetic phase, and T_c is a sizable fraction of the bandwidth. In this respect, FeSCs are often compared to the cuprates⁵², because the bandwidths are comparable. At a face value, $2\Delta_{\max}/T_c$ in underdoped cuprates is larger. However, one needs to take into account four additional considerations. First, the d -wave character of superconductivity in the cuprates modifies the $2\Delta_{\max}/T_c$ already in the BCS limit (Ref. [53]). Second, superconductivity in underdoped cuprates emerges from a pseudogap regime, and Δ_{\max} (the gap in the antinodal region) develops at an energy scale $T^* > T_c$. It would then be more appropriate to relate it to T^* rather than to T_c . Third, even above optimal doping, when pseudogap effects are relatively weak, phase fluctuations are not negligible, and the onset temperature T_p for the emergence of the bound pairs is larger than T_c . Eliashberg theory neglects phase fluctuations and, within it, one can only get the $2\Delta_{\max}/T_p$ ratio.

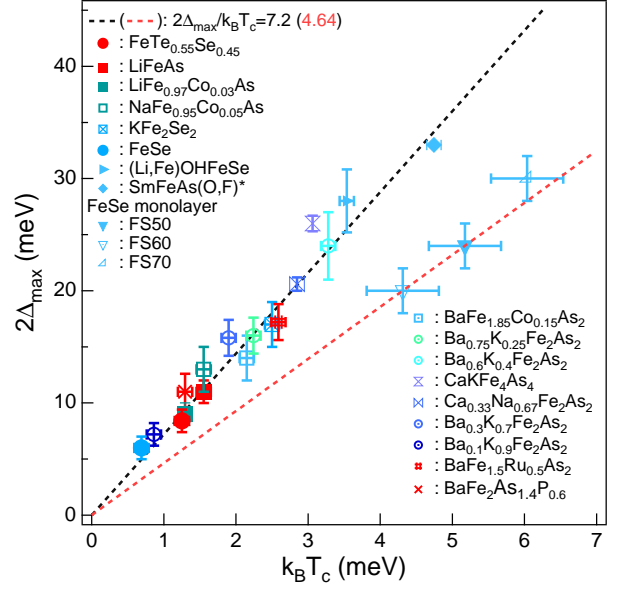


FIG. 5. (Color online) Summary of $2\Delta_{\max}^{\text{SC}}/k_B T_c$ that is determined by ARPES in various bulk FeSCs^{54–67} and monolayer FeSe films under different annealing conditions^{68,69}. The black and red dashed lines are linear function fit of the bulk FeSCs and monolayer FeSe, respectively. Since SmFeAs(O,F) has a non-neutral cleaved surface, the value of $2\Delta_{\max}^{\text{SC}}/k_B T_c$ is extracted from the bulk sensitive optical conductivity measurement⁷⁰. Systematic errors due to the finite instrumental resolution and the profile of the superconducting peak give 10%~17 % uncertainty of the $2\Delta_{\max}/k_B T_c$ values.

Fourth, there are substantial inhomogeneities in the sample, and one should compare a local temperature T_p and a local gap Δ_{\max} in a given region⁷¹. This has been done in the tunneling studies⁷², which reported $2\Delta_{\max}/T_p \sim 7.9$, not that far from FeSCs. If we take all this into consideration, it appears that FeSCs and the cuprates are closer than one would have expected at first sight.

The heavy fermion superconductors also have similar $2\Delta_{\max}/T_c$ ratios. For example, UPd₂Al₃ has $2\Delta_{\max}/T_c = 6$ ⁷³ and PuCoGa₅ has $2\Delta_{\max}/T_c = 6.4 \pm 0.4$ ⁷⁴, which give $\gamma \sim 1.0$. Notice that in these systems the Hund's coupling is important. On the other hand, the organic charge-transfer superconductors have ratios $2\Delta_{\max}/T_c = 4.8$ corresponding to $\gamma \sim 0.5$ ⁷⁵, which are believed to be Mott systems and the Hund's physics is not relevant.

Finally, we comment on earlier realistic calculations of superconductivity in FeSCs. Yin *et al.* investigated possible pairing states using the LDA+DMFT effective pairing interaction which describes the observed spectra⁷⁶. Because of the computational cost, they could not go to low enough temperatures to study $2\Delta_{\max}/T_c$ and/or carry out an Eliashberg treatment. Nourafkan *et al.* solved the Eliashberg equations but replaced frequency-dependent interaction by a constant⁷⁷. Ummarino carried out an Eliashberg treatment to FeSCs and yields similar $2\Delta_{\max}/T_c$ ratios as ours⁷⁸. In his work, the pairing

interaction was introduced phenomenologically. Combining the realistic pairing interaction with the Eliashberg approach is an outstanding challenge for future work.

Conclusions In this work, we build on the recent understanding of the physics of the Hund's metal and studied a phenomenological γ -model describing the superconductivity mediated by bosonic propagator with a power-law frequency dependence, $\lambda(\Omega) \propto 1/|\Omega|^\gamma$. This model captures the essence of the transition from a Hund's metal to a superconductor at a temperature comparable to or higher than a crossover temperature between non-Fermi-liquid and Fermi-liquid behavior^{9,11}.

We use the model to explore the main characteristics of the pairing gap and T_c , ignoring the complications such as the multiorbital or multiband structure of FeSCs. We find $2\Delta_{\max}/T_c$ to be independent of the interaction strength and equal to $7.2 - 7.3$ if we use $\gamma = 1.2$ obtained from the three-band Hubbard model. These results are in surprisingly good agreement with recent experiments which argued that $2\Delta_{\max}/T_c \approx 7.2$ is the same in at least two FeSCs: LiFeAs and FeTe_{0.55}Se_{0.45}¹⁴. It would be interesting to extend these observations to a more

realistic description of the materials, taking into account the multiorbital nature of the problem, and the fact that, in Hund's metals, the power-law behavior of local spin susceptibility holds in an intermediate temperature range between a Fermi-liquid regime at low temperatures and a high temperature regime where the orbitals and the spins are both quasi-atomic-like.

ACKNOWLEDGMENTS

We would like to thank Ar. Abanov, K. Haule, K. Stadler, J. VonDelft, and Y. Wu for numerous discussions on the subject of Hund's metals and superconductivity in the γ -model. T.-H.L. and G.K. were supported by the NSF Grant No. DMR-1733071. A.V.C. was supported by the NSF Grant No. DMR-1523036. H. M. is supported by the U.S. Department of Energy, Office of Basic Energy Sciences, Early Career Award Program under Award No. 1047478.

-
- ¹ Y. Kamihara, T. Watanabe, M. Hirano, and H. Hosono, *Journal of the American Chemical Society* **130**, 3296 (2008).
 - ² J. Paglione and R. L. Greene, *Nature Physics* **6**, 645 (2010).
 - ³ D. C. Johnston, *Advances in Physics* **59**, 803 (2010).
 - ⁴ Q. Si and E. Abrahams, *Phys. Rev. Lett.* **101**, 076401 (2008).
 - ⁵ P. Werner, E. Gull, M. Troyer, and A. J. Millis, *Phys. Rev. Lett.* **101**, 166405 (2008).
 - ⁶ K. Haule and G. Kotliar, *New Journal of Physics* **11**, 025021 (2009).
 - ⁷ A. Georges, L. de' Medici, and J. Mravlje, *Annual Review of Condensed Matter Physics* **4**, 137 (2013).
 - ⁸ Z. P. Yin, K. Haule, and G. Kotliar, *Nature Materials* **10**, 932 (2011).
 - ⁹ Z. P. Yin, K. Haule, and G. Kotliar, *Phys. Rev. B* **86**, 195141 (2012).
 - ¹⁰ C. Aron and G. Kotliar, *Phys. Rev. B* **91**, 041110 (2015).
 - ¹¹ K. M. Stadler, Z. P. Yin, J. von Delft, G. Kotliar, and A. Weichselbaum, *Phys. Rev. Lett.* **115**, 136401 (2015).
 - ¹² V. K. Thorsmølle, M. Khodas, Z. P. Yin, C. Zhang, S. V. Carr, P. Dai, and G. Blumberg, *Phys. Rev. B* **93**, 054515 (2016).
 - ¹³ A. Charnukha, Z. P. Yin, Y. Song, C. D. Cao, P. Dai, K. Haule, G. Kotliar, and D. N. Basov, *Phys. Rev. B* **96**, 195121 (2017).
 - ¹⁴ H. Miao, W. H. Brito, Z. P. Yin, R. D. Zhong, G. D. Gu, P. D. Johnson, M. P. M. Dean, S. Choi, G. K. Kotliar, W. Ku, X. C. Wang, C. Q. Jin, S. F. Wu, T. Qian, and H. Ding, *arXiv:1804.07601* (2018).
 - ¹⁵ Z. Wang, H. Yang, D. Fang, B. Shen, Q.-H. Wang, L. Shan, C. Zhang, P. Dai, and H.-H. Wen, *Nature Physics* **9**, 42 (2012).
 - ¹⁶ M. Eschrig, *Advances in Physics* **55**, 47 (2006).
 - ¹⁷ J. Mravlje and A. Georges, *Phys. Rev. Lett.* **117**, 036401 (2016).
 - ¹⁸ J. Mravlje, M. Aichhorn, T. Miyake, K. Haule, G. Kotliar, and A. Georges, *Phys. Rev. Lett.* **106**, 096401 (2011).
 - ¹⁹ H. T. Dang, J. Mravlje, A. Georges, and A. J. Millis, *Phys. Rev. Lett.* **115**, 107003 (2015).
 - ²⁰ H. T. Dang, J. Mravlje, A. Georges, and A. J. Millis, *Phys. Rev. B* **91**, 195149 (2015).
 - ²¹ X. Deng, K. Haule, and G. Kotliar, *Phys. Rev. Lett.* **116**, 256401 (2016).
 - ²² A. Abanov, A. V. Chubukov, and J. Schmalian, *Advances in Physics* **52**, 119 (2003).
 - ²³ A. V. Chubukov, D. Pines, and J. Schmalian, *The Physics of Superconductors, Vol. 1* (Springer, Berlin (edited by K. H. Bennemann and J. B. Ketterson), 2003) p. p. 495.
 - ²⁴ A. Abanov, A. V. Chubukov, and A. M. Finkel'stein, *EPL (Europhysics Letters)* **54**, 488 (2001).
 - ²⁵ A. Abanov, A. V. Chubukov, and M. R. Norman, *Phys. Rev. B* **78**, 220507 (2008).
 - ²⁶ E.-G. Moon and A. Chubukov, *Journal of Low Temperature Physics* **161**, 263 (2010).
 - ²⁷ Y. Wang, A. Abanov, B. L. Altshuler, E. A. Yuzbashyan, and A. V. Chubukov, *Phys. Rev. Lett.* **117**, 157001 (2016).
 - ²⁸ J.-H. She, B. J. Overbosch, Y.-W. Sun, Y. Liu, K. E. Schalm, J. A. Mydosh, and J. Zaanen, *Phys. Rev. B* **84**, 144527 (2011).
 - ²⁹ E. G. Moon and S. Sachdev, *Phys. Rev. B* **80**, 035117 (2009).
 - ³⁰ M. A. Metlitski, D. F. Mross, S. Sachdev, and T. Senthil, *Phys. Rev. B* **91**, 115111 (2015).
 - ³¹ H. Wang, S. Raghu, and G. Torroba, *Phys. Rev. B* **95**, 165137 (2017).
 - ³² See supplemental material for further details.
 - ³³ P. J. Hirschfeld, M. M. Korshunov, and I. I. Mazin, *Reports on Progress in Physics* **74**, 124508 (2011).
 - ³⁴ A. V. Chubukov, *Iron-based Superconductivity* (Springer Series in Materials Science (edited by D. P. Johnson, G.

- Xu, and W.-G. Yin), 2105) pp. 255–329.
- ³⁵ L. de Medici, *Iron-based Superconductivity* (Springer Series in Materials Science (edited by D. P. Johnson, G. Xu, and W.-G. Yin), 2105) pp. 409–441.
 - ³⁶ E. Bascones, B. Valenzuela, and M. J. Calderin, *Comptes Rendus Physique* **17**, 36 (2016).
 - ³⁷ R. M. Fernandes and A. V. Chubukov, *Reports on Progress in Physics* **80**, 014503 (2017).
 - ³⁸ G. Eliashberg, *Sov. Phys. JETP* **11**, 696 (1960).
 - ³⁹ R. Combescot, *Phys. Rev. B* **51**, 11625 (1995).
 - ⁴⁰ N. E. Bonesteel, I. A. McDonald, and C. Nayak, *Phys. Rev. Lett.* **77**, 3009 (1996).
 - ⁴¹ A. V. Chubukov, A. M. Finkel'stein, R. Haslinger, and D. K. Morr, *Phys. Rev. Lett.* **90**, 077002 (2003).
 - ⁴² A. Klein, S. Lederer, D. Chowdhury, E. Berg, and A. Chubukov, *Phys. Rev. B* **97**, 155115 (2018).
 - ⁴³ B. L. Altshuler, L. B. Ioffe, and A. J. Millis, *Phys. Rev. B* **50**, 14048 (1994).
 - ⁴⁴ R. Roussev and A. J. Millis, *Phys. Rev. B* **63**, 140504 (2001).
 - ⁴⁵ D. T. Son, *Phys. Rev. D* **59**, 094019 (1999).
 - ⁴⁶ A. V. Chubukov and J. Schmalian, *Phys. Rev. B* **72**, 174520 (2005).
 - ⁴⁷ J. Fink, A. Koitzsch, J. Geck, V. Zabolotnyy, M. Knupfer, B. Büchner, A. Chubukov, and H. Berger, *Phys. Rev. B* **74**, 165102 (2006).
 - ⁴⁸ A. Aperis and P. M. Oppeneer, *Phys. Rev. B* **97**, 060501 (2018).
 - ⁴⁹ J. J. Lee, F. T. Schmitt, R. G. Moore, S. Johnston, Y. T. Cui, W. Li, M. Yi, Z. K. Liu, M. Hashimoto, Y. Zhang, D. H. Lu, T. P. Devereaux, D. H. Lee, and Z. X. Shen, *Nature* **515**, 245 EP (2014).
 - ⁵⁰ S. Coh, M. L. Cohen, and S. G. Louie, *New Journal of Physics* **17**, 073027 (2015).
 - ⁵¹ C. Zhang, Z. Liu, Z. Chen, Y. Xie, R. He, S. Tang, J. He, W. Li, T. Jia, S. N. Rebec, E. Y. Ma, H. Yan, M. Hashimoto, Donghui, S.-K. Mo, Y. Hikita, R. G. Moore, H. Y. Hwang, D. Lee, and Z. Shen, *Nature Communications* **8**, 14468 (2017).
 - ⁵² D. N. Basov and A. V. Chubukov, *Nature Physics* **7**, 272 (2011).
 - ⁵³ K. A. Musesian, J. Betouras, A. V. Chubukov, and R. Joynt, *Phys. Rev. B* **53**, 3598 (1996).
 - ⁵⁴ K. Terashima, Y. Sekiba, J. H. Bowen, K. Nakayama, T. Kawahara, T. Sato, P. Richard, Y.-M. Xu, L. J. Li, G. H. Cao, Z.-A. Xu, H. Ding, and T. Takahashi, *Proceedings of the National Academy of Sciences* **106**, 7330 (2009).
 - ⁵⁵ K. Nakayama, T. Sato, P. Richard, Y.-M. Xu, T. Kawahara, K. Umezawa, T. Qian, M. Neupane, G. F. Chen, H. Ding, and T. Takahashi, *Phys. Rev. B* **83**, 020501 (2011).
 - ⁵⁶ X.-P. Wang, T. Qian, P. Richard, P. Zhang, J. Dong, H.-D. Wang, C.-H. Dong, M.-H. Fang, and H. Ding, *EPL (Europhysics Letters)* **93**, 57001 (2011).
 - ⁵⁷ N. Xu, P. Richard, X.-P. Wang, X. Shi, A. van Roeyeghem, T. Qian, E. Ieki, K. Nakayama, T. Sato, E. Rienks, S. Thirupathiah, J. Xing, H.-H. Wen, M. Shi, T. Takahashi, and H. Ding, *Phys. Rev. B* **87**, 094513 (2013).
 - ⁵⁸ Z.-H. Liu, P. Richard, K. Nakayama, G.-F. Chen, S. Dong, J.-B. He, D.-M. Wang, T.-L. Xia, K. Umezawa, T. Kawahara, S. Souma, T. Sato, T. Takahashi, T. Qian, Y. Huang, N. Xu, Y. Shi, H. Ding, and S.-C. Wang, *Phys. Rev. B* **84**, 064519 (2011).
 - ⁵⁹ H. Miao, P. Richard, Y. Tanaka, K. Nakayama, T. Qian, K. Umezawa, T. Sato, Y.-M. Xu, Y. B. Shi, N. Xu, X.-P. Wang, P. Zhang, H.-B. Yang, Z.-J. Xu, J. S. Wen, G.-D. Gu, X. Dai, J.-P. Hu, T. Takahashi, and H. Ding, *Phys. Rev. B* **85**, 094506 (2012).
 - ⁶⁰ H. Miao, T. Qian, X. Shi, P. Richard, T. K. Kim, M. Hoesch, L. Y. Xing, X.-C. Wang, C.-Q. Jin, J.-P. Hu, and H. Ding, *Nature Communications* **6**, 6056 (2015).
 - ⁶¹ H. Miao, Z. P. Yin, S. F. Wu, J. M. Li, J. Ma, B.-Q. Lv, X. P. Wang, T. Qian, P. Richard, L.-Y. Xing, X.-C. Wang, C. Q. Jin, K. Haule, G. Kotliar, and H. Ding, *Phys. Rev. B* **94**, 201109 (2016).
 - ⁶² Y.-B. Shi, Y.-B. Huang, X.-P. Wang, X. Shi, A.-V. Roeyeghem, W.-L. Zhang, N. Xu, P. Richard, T. Qian, E. Rienks, S. Thirupathiah, K. Zhao, C.-Q. Jing, M. Shi, and H. Ding, *Chinese Physics Letters* **31**, 067403 (2014).
 - ⁶³ D. Mou, T. Kong, W. R. Meier, F. Lochner, L.-L. Wang, Q. Lin, Y. Wu, S. L. Bud'ko, I. Eremin, D. D. Johnson, P. C. Canfield, and A. Kaminski, *Phys. Rev. Lett.* **117**, 277001 (2016).
 - ⁶⁴ H. Ding, P. Richard, K. Nakayama, K. Sugawara, T. Arakane, Y. Sekiba, A. Takayama, S. Souma, T. Sato, T. Takahashi, Z. Wang, X. Dai, Z. Fang, G. F. Chen, J. L. Luo, and N. L. Wang, *EPL (Europhysics Letters)* **83**, 47001 (2008).
 - ⁶⁵ N. Xu, P. Richard, X. Shi, A. van Roeyeghem, T. Qian, E. Razzoli, E. Rienks, G.-F. Chen, E. Ieki, K. Nakayama, T. Sato, T. Takahashi, M. Shi, and H. Ding, *Phys. Rev. B* **88**, 220508 (2013).
 - ⁶⁶ Y. Zhang, Z. R. Ye, Q. Q. Ge, F. Chen, J. Jiang, M. Xu, B. P. Xie, and D. L. Feng, *Nature Physics* **8**, 371 (2012).
 - ⁶⁷ D. Liu, C. Li, J. Huang, B. Lei, L. Wang, X. Wu, B. Shen, Q. Gao, Y. Zhang, X. Liu, Y. Hu, Y. Xu, A. Liang, J. Liu, P. Ai, L. Zhao, S. He, L. Yu, G. Liu, Y. Mao, X. Dong, X. Jia, F. Zhang, S. Zhang, F. Yang, Z. Wang, Q. Peng, Y. Shi, J. Hu, T. Xiang, X. Chen, Z. Xu, C. Chen, and X. J. Zhou, *arXiv:1802.02940* **106**, 7330 (2018).
 - ⁶⁸ J. J. Lee, F. T. Schmitt, R. G. Moore, S. Johnston, Y.-T. Cui, W. Li, M. Yi, Z. K. Liu, M. Hashimoto, Y. Zhang, D. H. Lu, T. P. Devereaux, D.-H. Lee, and Z.-X. Shen, *Nature* **515**, 245 (2014).
 - ⁶⁹ X. Shi, Z.-Q. Han, X.-L. Peng, P. Richard, T. Qian, X.-X. Wu, M.-W. Qiu, S. C. Wang, J. P. Hu, Y.-J. Sun, and H. Ding, *Nature Communications* **8**, 14988 (2017).
 - ⁷⁰ A. Charnukha, D. Präpper, N. D. Zhigadlo, M. Naito, M. Schmidt, Z. Wang, J. Deisenhofer, A. Loidl, B. Keimer, A. V. Boris, and D. N. Basov, *Phys. Rev. Lett.* **120**, 087001 (2018).
 - ⁷¹ D. Pelc, P. Popevi, G. Yu, M. Poek, G. M., and N. Bari, *arXiv:1710.10221* (2017).
 - ⁷² K. K. Gomes, A. N. Pasupathy, A. Pushp, S. Ono, Y. Ando, and A. Yazdani, *Nature* **447**, 569 (2007).
 - ⁷³ N. K. Sato, N. Aso, K. Miyake, R. Shiina, P. Thalmeier, G. Varelogiannis, C. Geibel, F. Steglich, P. Fulde, and T. Komatsubara, *Nature* **410**, 340 (2001).
 - ⁷⁴ D. Daghero, M. Tortello, G. Ummarino, J.-C. Griveau, E. Colineau, R. Eloirdi, A. Shick, J. Kolorenc, A. Liechtenstein, and R. Caciuffo, *Nature Communications* **3**, 786 (2012).
 - ⁷⁵ R. Lortz, Y. Wang, A. Demuer, P. H. M. Böttger, B. Bergk, G. Zwicknagl, Y. Nakazawa, and J. Wosnitza, *Phys. Rev. Lett.* **99**, 187002 (2007).
 - ⁷⁶ Z. P. Yin, K. Haule, and G. Kotliar, *Nature Physics* **10**, 845 (2014).
 - ⁷⁷ R. Nourafkan, G. Kotliar, and A.-M. S. Tremblay, *Phys.*

Rev. Lett. **117**, 137001 (2016).

⁷⁸ G. A. Ummarino, Phys. Rev. B **83**, 092508 (2011).

Supplemental Materials: Pairing Mechanism in Hunds Metal Superconductors and the Universality of the Superconducting Gap to Critical Temperature Ratio

I. SPIN-FLUCTUATION ELIASHBERG THEORY

The Eliashberg equations after averaging over the Fermi surface reads^{23,26,46},

$$Z(\omega_n) = 1 + \pi T \sum_m \frac{\omega_m}{\omega_n} \lambda(\omega_m - \omega_n) \frac{Z(\omega_m)}{\sqrt{Z(\omega_m)^2 \omega_m^2 + \Phi(\omega_m)^2}}, \quad (\text{S1})$$

$$\Phi(\omega_n) = Z(\omega_n) \Delta(\omega_n) = \pi T \sum_m \lambda(\omega_m - \omega_n) \frac{\Phi(\omega_m)}{\sqrt{Z(\omega_m)^2 \omega_m^2 + \Phi(\omega_m)^2}}, \quad (\text{S2})$$

where $Z(\omega_n) = 1 + \frac{\Sigma(\omega_n)}{\omega_n}$ is the quasiparticle renormalization factor, $\Delta(\omega_n)$ is the pairing gap, and $\Sigma(\omega)$ and $\Phi(\omega_n)$ is the normal and anomalous self-energy, respectively. The pairing interaction is defined as

$$\lambda(\Omega_n) = gN(0)\chi'_{loc}(\Omega_n) = \int_0^\infty d\nu \frac{2g\nu N(0)}{\Omega_n^2 - \nu^2} \chi''_{loc}(\nu), \quad (\text{S3})$$

where $\chi_{loc}(\omega_n - \omega_m) \equiv \int_0^{2k_F} dq q \chi(q, \omega_n - \omega_m)$ is the local spin susceptibility⁴⁶ and we use the spectral representation of the susceptibility.

Combining Eq. S1 and Eq. S2, we are left with only one self-consistent equation,

$$\Delta(\omega_n) = \pi T \sum_m \frac{\lambda(\omega_m - \omega_n)}{\sqrt{\omega_m^2 + \Delta^2(\omega_m)}} (\Delta(\omega_m) - \Delta(\omega_n) \frac{\omega_m}{\omega_n}), \quad (\text{S4})$$

and the quasiparticle renormalization factor can be calculated from

$$\omega_n Z(\omega_n) = \omega_n + \pi T \sum_m \lambda(\omega_m - \omega_n) \frac{\omega_m}{\sqrt{\omega_m^2 + \Delta^2(\omega_m)}}. \quad (\text{S5})$$

II. THE POWER LAW-BEHAVIOR IN THE SPIN-EXCITATION OF HUND'S METALS

In this section, we show the power-law behavior in the spin-excitation of Hund's metals based on the data in the Fig. 3(c) of Ref. 11 and our continuous-time quantum Monte-Carlo (CTQMC) simulation, and their relation to the pairing interaction, $\lambda(\Omega_n)$, as defined in Eq. S3.

Fig. S1 shows the local spin susceptibility of the three-band Hubbard model, which captures the essence of Hund's physics, extracted from the Fig. 3(c) of Ref. 11. The vertical solid and dashed line in Fig. S1 denote the spin Kondo temperature, T_K^{sp} , and orbital Kondo temperature, T_K^{orb} , respectively. Below T_K^{sp} , both the spin and orbital degrees of freedom are screened. Therefore, the system shows a Fermi-liquid behavior characterized by a linear susceptibility, $\chi''(\omega) \propto \omega$. In the intermediate regime, $T_K^{sp} < \omega < T_K^{orb}$, the screened orbital degrees of freedom coupled to the slow fluctuating spins leading to a fractional power-law behavior in the spin-excitation as indicated by the fit to $\chi''(\omega) \propto \omega^{-1.2}$. The energy scale in this intermediate regime is pertinent to the superconducting temperature of the iron-based superconductors. Therefore, the fractional spin-excitation may mediate the pairing of the superconductivity. Having established the fractional power of the spin-excitation, it is straightforward to show from Eq. S3 that the pairing interaction has the form $\lambda(\Omega_n) \propto |\Omega_n|^{-1.2}$ given that $\chi''(\omega) \propto \text{sign}(\omega)|\omega|^{-1.2}$.

In Fig. S2(a), we also present the z-component of the local spin susceptibility, $\chi'_{zz,loc}(\Omega_n)$, from our continuous-time quantum Monte Carlo (CTQMC) simulation on three-band Hubbard model, where we set the hopping, $t = 1$, as our unit of energy, the Coulomb interaction, Hund's coupling interaction and the chemical potential are set to $U = 5$, $J = 1$, and $\mu = 7.032$, respectively (the same setting as in Fig. 1 of Ref. 11). The temperature, however, is set to $T = 0.002t$, which corresponds to $T = 10K$ if we set $t = 0.5$ eV. The local spin susceptibility shows a power-law

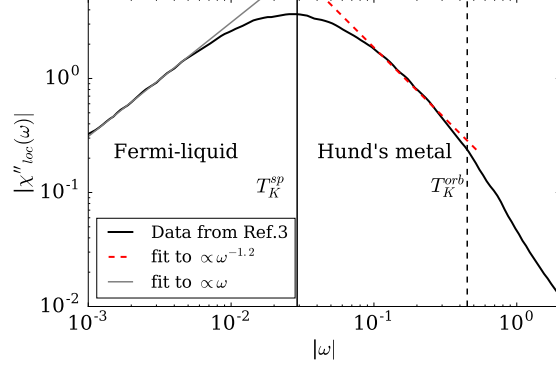


FIG. S1. The local spin susceptibility, $\chi''_{loc}(\omega)$, for three-band Hubbard model at $T = 0.001t$ extracted from Fig. 3(c) of Ref. 11.

behavior, $\chi'_{zz,loc}(\Omega_n) \propto |\Omega_n|^{-1.2}$, in the intermediate energy scale and saturate to a constant at low temperature. Note that the temperature is slightly higher than the one in Fig. S1 so the Fermi liquid behavior (saturation to a constant susceptibility) is not fully established. From Eq. S3, it is straightforward to show that $\lambda(\Omega_n) \propto |\Omega_n|^{-1.2}$ given that $\chi'_{zz,loc}(\Omega_n) \propto |\Omega_n|^{-1.2}$, where we use the fact that $\chi'_{zz,loc}(\Omega_n) \approx \chi'_{loc}(\Omega_n)$ in our rotationally-invariant three-band Hubbard model. Figure S2(b) shows the imaginary part of the self-energy, $Im\Sigma(\omega_n)$, with the same parameter setting as in Fig. S2(a). A fractional power-law behavior, $Im\Sigma(\omega_n) \propto \omega_n^{0.46}$, also exist in the intermediate energy. At low temperature, the Fermi-liquid behavior, $Im\Sigma(\omega_n) \propto \omega_n$, is recovered.

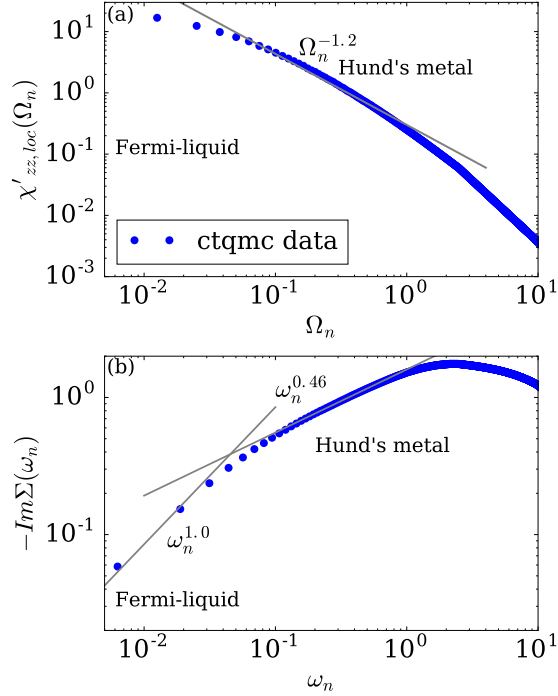


FIG. S2. (a) The z-component of the local spin susceptibility, $\chi'_{zz,loc}(\Omega_n)$, from CTQMC simulation on three-band Hubbard model at $T = 0.002t$, $U = 5t$, $J = 1t$, and $\mu = 7.032t$ where t is the hopping amplitude (the same setting as in Fig. 1 of Ref. 11). (b) The imaginary part of the self-energy, $Im\Sigma(\omega_n)$, with the same parameters.